

Multi-Fingered Active Grasp Learning

Qingkai Lu¹, Mark Van der Merwe¹, and Tucker Hermans¹

Abstract—Learning-based approaches to grasp planning are preferred over analytical methods due to their ability to better generalize to new, partially observed objects. However, data collection remains one of the biggest bottlenecks for grasp learning methods, particularly for multi-fingered hands. The relatively high dimensional configuration space of the hands coupled with the diversity of objects common in daily life requires a significant number of samples to produce robust and confident grasp success classifiers. In this paper, we present the first active learning approach to grasping that searches over the grasp configuration space and classifier confidence in a unified manner. Our real-robot grasping experiment shows our active grasp planner using less training data achieves comparable success rates with a passive supervised planner trained with geometrical grasping data. We also compute the differential entropy to demonstrate our active learner generates grasps with larger diversity than passive supervised learning using more heuristic data. We base our approach on recent success in planning multi-fingered grasps as probabilistic inference with a learned neural network likelihood function. We embed this within a multi-armed bandit formulation of sample selection. We show that our active grasp learning approach uses fewer training samples to produce grasp success rates comparable with the passive supervised learning method trained with grasping data generated by an analytical planner.

I. INTRODUCTION

Learning-based grasp planning [1–9] has become popular over the past decade, because of its ability to generalize well to novel objects with only partial-view object information [10]. These approaches require large amounts of data for training, particularly those that utilize deep neural networks [8, 9, 11–13]. However, large scale data collection remains a challenge for multi-fingered grasping, because (1) objects common in daily life exhibit large variation in terms of geometry, texture, inertial properties, and appearance; and (2) the relatively high dimension of multi-fingered grasp configurations, (e.g. 22 dimensions for the configuration of Allegro hand in Cartesian space and 23 in the LBR4 arm joint configuration space).

Random sampling is a common approach for data collection of two-finger gripper grasping [5, 7, 14]. Considering the sparsity of successful grasps in the high dimensional configuration space of multi-fingered grasping, it is not practical to collect enough successful grasps using random sampling. Eppner et al. [15] exhaustively sample more than 1 billion grasps for each of 21 objects from the YCB data set to improve the understanding of data generation for 6-DOF, parallel jaw grasp learning algorithms. However, this approach would not scale well to multi-fingered grasping due to its high dimensionality. All existing deep learning work [8, 11, 12] for multi-fingered grasping collect training grasps using an analytical grasp planner. However, analytical grasp planners bias data collection to only cover a subspace

of feasible grasp configurations such as force closure and cannot guarantee generating successful grasps for an arbitrary training object.

Traditional passive supervised grasp learning learns well over the space covered by the training data, but has limited power to explore and generalize to the space not covered by the training data. This is especially true for novel objects. We propose an active learning approach to interactively learn a grasp model that better covers the grasp configuration space across different objects using fewer samples compared with passive supervised grasp learning. Instead of passively inducing a hypothesis to explain the available training data as in standard supervised learning, active learning develops and tests new hypotheses continuously and interactively. Active learning is most appropriate when 1) unlabeled data samples are numerous, 2) a lot of labeled data are needed to train an accurate supervised learning system, and 3) data samples can be easily collected or synthesized [16]. Grasp learning satisfies each of these conditions: 1) there are infinitely many possible grasps, 2) a large number of labeled training samples are necessary to cover the space [15], and 3) the robot is its own oracle - it can label grasps by trying them and automatically detecting success or failure without human labeling.

We propose modeling active grasp learning as a multi-armed bandit problem, which is designed to improve the grasp success classifier and enable the grasp model to cover the space of grasp configurations and objects as much as possible. Our proposed method is fundamentally different from existing bandit-based grasping work [17–19], which treat each possible grasp as one arm and perform grasp planning separately for different objects. We instead use the bandit-framework to select qualitatively different grasps to actively improve our grasp model in a unified manner across all objects in our training set.

We perform grasp planning as probabilistic inference using our actively learned grasp model to generate high-quality grasps for objects with different shapes and textures. Our work demonstrates the first deep, active learning approach to robotic grasping. Our real-robot grasping experiments show our active grasp planner achieves comparable success rates, while using fewer training data, when compared to a passive supervised planner [8, 13, 20] trained on data generated with a geometric grasp planner. We also demonstrate our active learning is able to generate grasps with larger diversity.

In the next section we review the literature of grasp planning and active learning in robotic grasping. In Section III we introduce our grasp planning as inference framework and define our grasp model. We then describe our novel bandit-

based active grasp learning algorithm in Section IV and our online model update algorithm for active grasp learning in Section V. In Section VI, we give a thorough account of our experimental evaluation. In Section VII, we conclude with a brief discussion and suggest directions for future work.

II. RELATED WORK

Broadly speaking, deep grasp learning methods either predict grasp success from an image patch associated with a grasp configuration [4, 5, 7, 9, 11, 14, 21, 22], or directly predicts a grasp configuration from an image or image patch using regression [12, 23, 24]. Most deep grasp learning approaches such as [1, 4–7, 9, 25] focus on parallel jaw grippers, while relatively little work has focused on the more difficult multi-fingered grasping problem [8, 11–13, 26]. Deep learning requires large amount of training data, however, it is challenging to collect a large amount of grasp training data, especially for multi-fingered grasping. Dexnet [7] generated 6.7 million synthetic training grasps over 1,500 3D mesh models for two-fingered parallel jaw grippers using the force closure [27] metric. Levine et al. [14] and Pinto et al. [5] collected 800,000 and 50,000 two-fingered grasps respectively by generating and executing heuristic grasps in clutter and label them automatically on real robots with parallel jaw grippers. Compared with grasp training data of two-fingered parallel jaw grippers, it is more difficult to collect grasping data for multi-fingered hand. 3,770 grasps were generated for the Barrett hand using GraspIt! [28] in [11]. Lu et al. [8] collected 1507 grasps for the Allegro hand in simulation using a primitive-based geometric planner. Veres et al. [12] collected a data-set of around 47,000 grasps for the Barrett hand using a geometrical planner in simulation. In this paper, we propose a novel active grasp learning approach to address the data collection bottleneck for grasp learning.

Kroemer et al. [17] combine active learning and reactive control for robot grasping. A grasp is represented as the 6 DOF hand pose of the hand preshape. Grasp learning and experiments are performed separately for different objects, which means the learning does not share information across different objects. In [29], an active learning approach is presented for assessing robot grasp reliability. Each grasp is represented as a 9-dimensional feature derived from a set of grasp quality criteria. It classifies grasp success using the weighted k-nearest neighbors and defines a classification confidence metric for the pooling-based active learning. A grasp dataset containing more than 900 grasps over 4 different objects for the Barrett hand is collected. The collected grasp dataset is split into a validation for evaluation and a pool set for active learning. The grasp active learning in [29] is not evaluated as a pure classification problem without performing grasp planning.

Montesano et al. [30] address the problem of actively learning good grasping points in a pooling way to reduce the number of examples needed for training the grasping model.

This paper combines beta-binomial distributions and a non-parametric kernel approach to compute the success probability of grasping points. Its proposed active learning metric favors the exploration of these areas with high probability of success or where uncertainty is high. This pooling-based active learning is tested on a real humanoid robot for both seen and unseen objects. In [31], active perception is used to collect the training data set efficiently. for each specific object. Tian et al. [32] present bijective contact mapping for transferring grasp contact points from an example object to a novel object.

Existing bandit-based grasping work [17–19] treats each possible grasp as one arm and perform grasp planning separately for different objects. Instead, we use the bandit-framework to select qualitatively different grasps to actively improve our grasp deep learning models in a unified manner across all objects in our training set. Moreover, none of these multi-armed bandit grasp planning work focus on rigid multi-fingered hand grasping like we do. In [17], active grasp learning for the Barrett hand is formulated as a continuum-armed bandits problem by treating each grasp pose as one arm. A continuum Gaussian Bandits algorithm is proposed to solve the continuum-armed bandits problem. For the Continuum Gaussian Bandits algorithm, the local maxima is detected using a gradient based method inspired from mean shift.

In [18, 33], multi-armed bandit is used to generate force closure grasps for parallel jaw grippers on each given 2D planar object. Mahler et al. [19] extends the multi-armed bandit grasp planning of [18] from 2D to 3D objects for parallel jaw grippers. The similarity between a pair of grasps and objects is measured and used as the prior information for the multi-armed bandit grasp planning. The object feature is extracted using a Multi-View CNN. Thompson sampling is used to solve the grasping multi-armed bandit problem in [18, 19, 33]. Oberlin et al. [34] formalize grasping for parallel jaw grippers as a multi-armed bandit problem. It defines a new algorithm called Prior Confidence Bound for best arm identification in budgeted bandits, which enables the robot to quickly find an arm corresponding to a good grasp without pulling all the arms. A linear grasp model is used to score grasp candidates for their grasping multi-armed bandit. They take an instance-based approach that needs to collect training data for all testing objects to be grasped, which does not generalize to novel objects.

In [35], context multi-armed bandit is applied to select one of three pre-defined environment-constrained grasping strategies for a given object, instead of learning the grasp configuration across different objects like we do. Different multi-armed bandit algorithms such as Thompson sampling and GP-UCB are experimented in [35].

Compared with existing grasp active learning work, our active learning approach has three novelties: the first grasp active learning work leveraging deep networks; doing a continuous synthesis approach instead of pooling for grasp active

learning; modeling grasp active learning as a multi-armed bandit problem to cover the grasp space across different objects efficiently.

III. GRASP PLANNING AS INFERENCE

We define the grasp planning problem as finding a grasp preshape configuration following [28]. In our case, the grasp configuration vector is composed of the palm pose in the object reference frame and the hand’s preshape joint angles that define the shape of the hand prior to closing the hand [13]. In order to make the grasp inference agnostic to object poses, we put the palm pose in the object reference frame for learning and inference.

After finding the grasp preshape configuration, the robot moves to this preshape and runs a controller to close the hand forming the grasp on the object. We explain the specific joints used for defining the preshape and how the grasp controller works for our experiments in Section VI-A. We focus on scenarios where a single, isolated object of interest is present in the scene. Importantly, we assume no explicit knowledge of the object beyond a single camera sensor reading of it in its current pose. The problem we address is, given such a grasp scenario, plan a grasp preshape configuration that allows the robot to successfully grasp and lift the object without dropping it.

At learning time, we learn the palm pose of the preshape in the Cartesian space. At inference time, we optimize the palm pose of the preshape in the arm joint configuration space, which means we solve the robot arm inverse kinematics as part of our grasp optimization. Learning in Cartesian space and planning in robot arm configuration space makes the grasp learning agnostic to different robot arms.

We use θ to represent the grasp configuration with the palm pose in Cartesian space. We use q to represent the grasp configuration with the palm pose in the robot arm joint configuration space.

Given the learned model parameters, W and Φ , along with the visual representation, z , associated with an observed object of interest, our goal is to infer the grasp configuration q in the robot arm joint configuration space that maximizes the posterior probability of grasp success $Y = 1$. Here Y defines a random Boolean variable with 0 meaning failure and 1 meaning success. We can thus formalize grasp planning as a *maximum a posteriori* (MAP) inference problem:

$$\begin{aligned} \operatorname{argmax}_q \quad & p(q|Y = 1, z, W, \Phi) \propto p(Y = 1|q, z, W)p(q|z, \Phi) \\ \text{subject to} \quad & q_{min} \leq q \leq q_{max} \end{aligned} \quad (1)$$

We constrain the grasp configuration parameters to obey the joint limits of the robot hand in Eq. 1.

We define the grasp success likelihood $p(Y = 1|\theta, z, W)$ to be a voxel-based 3D convolutional network following [13]. W represents the neural network parameters. The voxel-based network predicts the probability of grasp success, Y , as a function of the visual representation of the object

of interest, z , and grasp configuration in Cartesian space, θ . Figure 1a shows the architecture of our grasp success prediction network.

In order to model the grasp configuration distribution based on the geometry of the object of interest, we construct a mixture-density network (MDN) as our object conditional prior following [13]. Given its input an MDN predicts the parameters (means, covariance and mixing weights) of a Gaussian mixture model as output. Our MDN takes the visual representation of the object of interest z as input and predicts the parameters of a GMM modeling a probability distribution over grasp configurations. Thus the MDN learns to model the conditional probability distribution $p(\theta|z, \Phi)$ where Φ define the learned weights of the MDN. Figure 1b shows the architecture of our grasp success prediction network. We train our voxel-based MDN using the negative log likelihood loss.

We use the object voxel-grid and the object size vector as the visual object representation [13]. In order to generate the voxel-grid we first segment the object from the 3D point cloud by fitting a plane to the table using RANSAC and extracting the points above the table. We then estimate the first and second principle axes of the segmented object to create a right-handed object reference frame aligned relative to the world frame. We compute the object size along the three coordinates of the object reference frame to construct the object size vector. We then generate a $32 \times 32 \times 32$ voxel grid oriented about this reference frame. More details of the voxel-grid generation are described in [13].

We solve the grasp inference in the log-probability space and regularize the log-prior with a multiplicative gain of 0.5 to prevent the prior dominating the inference. We use the popular L-BFGS optimization algorithm with bound constraints to efficiently solve the inference problem. We use the scikit-learn¹ library to perform the optimization. We initialize the inference by randomly sampling from the MDN prior.

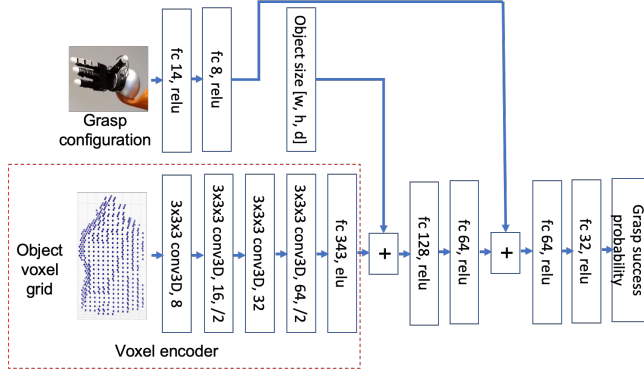
IV. ACTIVE GRASP LEARNING

The main scenarios that have been considered in active learning are stream-based selective sampling, pool-based sampling and query synthesis [16]. In this paper, we generate grasp query synthesis in a continuous fashion.

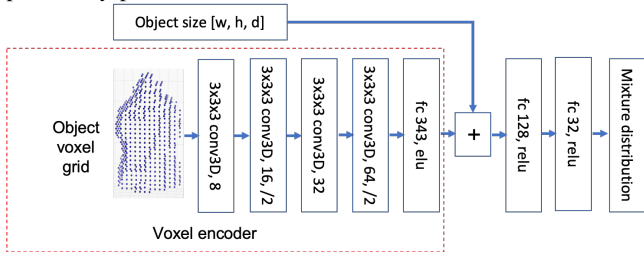
Multi-armed bandit is a classic reinforcement learning problem where we are given n slot machine (arms). Each slot machine has its probability distribution of reward. At each time step, the agent chooses one slot machine to play and receives a reward. The agent decides which arm to play at each time step such that it can maximize the accumulative reward.

We present three arms for our active learning: the likelihood uncertainty of the grasp success classifier, the grasp success probability maximization, and the grasp configuration exploration. These three arms are designed to improve the

¹<http://scikit-learn.org/stable/index.html>



(a) The architecture of our voxel-config-net for grasp success probability prediction.



(b) The architecture of our MDN modeling the grasp conditional prior.

Fig. 1: The voxel-config-net and MDN architectures [13]. Bottom left visualizes the voxel-grid for the “mustard bottle” object. All convolutional layers use $3 \times 3 \times 3$ 3D convolutional filters with exponential linear unit (ELU) activations. We annotate the number of filters and the stride (/2 means a stride of 2) for convolutional layers. We annotate the number of neurons and the activation function for fully connected layers.

grasp success classifier and enable the grasp model to cover the grasp configuration and object space as much as possible. We formulate active grasp learning as a multi-arm bandit problem to balance the exploration and exploitation of these three arms. We solve the bandit problem using the classical Upper Confidence Bound (UCB) algorithm. The UCB algorithm exploits actions with high average rewards obtained and explores more uncertain actions.

The grasp likelihood uncertainty maximization arm improves the grasp success classification, which is a common metric for active learning of binary classification problems.

$$\begin{aligned} \operatorname{argmax}_{\mathbf{q}} \quad & f(\mathbf{q}) + g(\mathbf{q}) \\ \text{subject to} \quad & \mathbf{q}_{\min} \leq \mathbf{q} \leq \mathbf{q}_{\max} \end{aligned} \quad (2)$$

$$f(\mathbf{q}) = \frac{1}{2(1 + \exp(-\log p(\mathbf{q}|z, \phi)))} \quad (3)$$

$$g(\mathbf{q}) = \begin{cases} p(Y = 1|\mathbf{q}, z, \mathbf{w}) & p(Y = 1|\mathbf{q}, z, \mathbf{w}) \leq 0.5 \\ 1 - p(Y = 1|\mathbf{q}, z, \mathbf{w}) & p(Y = 1|\mathbf{q}, z, \mathbf{w}) > 0.5 \end{cases} \quad (4)$$

Given the learned model parameters \mathbf{W} , Φ , and the visual representation z associated with an observed object of interest, our goal is to infer the grasp configuration parameters \mathbf{q} in the robot arm joint configuration space that maximize the likelihood uncertainty of grasp success Y . We represent the object of interest as a voxel-grid, as described in Section III. We define the likelihood uncertainty maximization arm in Eq 2. $f(\mathbf{q})$ in Eq 3 represents the grasp success classification uncertainty. $g(\mathbf{q})$ in Eq 4 regularizes the optimization to not stray into areas far from grasp configurations observed in the training data. We use L-BFGS with bound constraints to solve the uncertainty maximization initialized with a configuration sampled from the prior. We treat its optimized objective function value as its bandit reward.

Class imbalance is a common issue of grasp training data since it is harder to collect successful grasps than failure grasps. For example, only 11% out of 1507 training grasps in [8] are successful grasps. The grasp success probability maximization arm encourages the active learner to synthesize more successful grasps to overcome the grasp class imbalance issue. We perform the same grasp inference with the same objective function (Eq. 1) for the grasp success maximization arm. We normalize the logarithm of the optimized grasp success posterior with a Sigmoid function as its reward.

The grasp configuration exploration arm enables the grasp model to cover a larger portion of the grasp configuration space by exploring the areas it has less evidence of. We sample 50 grasp configuration candidates from the prior and select the one with lowest prior probability density as the grasp to explore. We compute the Sigmoid of the negative logarithm of the prior density as the reward of the selected grasp. We randomly select objects for active learning in order to cover the object space well.

V. ONLINE MODEL UPDATE

Cohn [36] evaluates both batch retraining and incremental online training for active learning of a single hidden layer neural network on the task of 2D planar arm kinematics learning. While the re-trained learner’s performance was slightly better in [36], their total training time was significantly longer than their incrementally trained counterparts. In [37], the deep network for active learning on image data is retrained after each active learning acquisition, which takes long training time. We use an incremental online update method for grasp active learning.

We train the initial grasp prediction network and MDN model for active learning using mini-batch gradient descent on the geometrical data set from [13] in a passive supervised way. We train our voxel-based prediction network and MDN using the Adam optimizer with mini-batches of size 64 for 90 epochs. The learning rate starts at 0.001 and decreases by $10 \times$ every 30 epochs. We pre-train the voxel encoder for our classifier and MDN on a voxel-based 3D object reconstruction task. We recommend readers to refer to [13] for more details of the initial grasp model training. Compared with the training in [13], the only difference in this paper

is we used layer norm instead of batch norm for both the prediction network and MDN.

For each round of active learning, we first apply the multi-arm bandit algorithm to generate an active learning mini-batch that contains 16 grasps using the model of previous round (i.e. data acquisition), then online update the grasp model, including the voxel-based classifier and the MDN prior. We online update the voxel-based grasp prediction network and the MDN prior using the Adam optimizer with mini-batches of size 16 and learning rate of $1e^{-5}$. We define every 4 consecutive active learning rounds to be a “meta-round”. For the first 3 rounds of the meta-round, we online update the voxel-based grasp prediction network and the MDN prior using the mini-batch data of the current active learning round for 5 epochs. For the last round of the meta-round, we online update the grasp prediction network and the MDN prior using all grasps, including all the geometrical and active learning grasps, for 5 epochs.

VI. EXPERIMENTS

In this section, we describe the experimental evaluation and analysis of our grasp active learning method. We compare our active learning approach to passive supervised learning approach used to initialize our active learning grasp model. We then compare to the passive supervised learning model with more training samples.

A. Robotic System for Data Collection and Experiments

We conduct all training and experiments using the four-fingered, 16 DOF Allegro hand mounted on a Kuka LBR4 7 DOF arm. We evaluate our grasp planners on the physical robot. We use a Kinect2 camera to generate the point cloud of the object on the table. One example RGB image of the robot and the object generated by Kinect2 can be seen from Figure 2. We collected simulated grasp data for grasp model training using our robot hand-arm setup inside the Gazebo simulator with the DART physics engine². We use the built-in Gazebo Kinect camera to generate point clouds simulating a Kinect2 RGB-D camera we use in real-world experiments. All data and software used in this paper are available online³.

We collected training data using a heuristic, geometry-based grasp planner in simulation in [13]. We generate a grasp preshape by randomly sampling joint angles for the first two joints of all fingers within a reasonable range, fixing the last two joints of each finger to be zero. We collected both multi-fingered side and overhead grasps. More details of our grasping data collection can be seen from [13].

There are 15 parameters for the Allegro hand preshape, 7 for the LBR4 arm joint angles representing the palm pose and 8 relating to the first 2 joint angles of each finger proximal to the palm. Given a desired arm joint configuration and preshape we use the RRT-connect motion planner in MoveIt! to plan a path for the arm. We execute all feasible plans moving the robot to the sampled preshape.



Fig. 2: Example RGB image of the experimental robot setup from the RGB-D Kinect 2 camera.

	Max success	Max uncertainty	Exploration
Average reward	0.965	0.922	0.933
Average time	8.11	4.15	2.53
Number of pulls	933	522	597

TABLE I: Average rewards and number of pulls for 3 active learning arms.

After moving the hand to the desired preshape, the robot runs a grasp controller to close the hand. The grasp controller closes the fingers at a constant velocity stopping each finger independently when contact is detected by the measured joint velocities being close to zero. The grasp controller closes the second and third joints of the non-thumb fingers and the two distal joints of the thumb. Note the proximal joint of all non-thumb fingers rotates the finger about its major axis causing it to change the direction of closing. As such we maintain the angle provided by the grasp planner for these joints. Upon closing, the robot attempts to lift the object to a height of 15cm. If the robot succeeds in reaching this height without the object falling, the simulator automatically labels the grasp as successful.

B. Active Learning Setup and Analysis

We train the initial grasp model, including the voxel-based classifier and the MDN conditional prior, for active learning in a passive supervised way, whose training specifications is mentioned in Section III. We collected 10 sets of grasps on Bigbird objects data set [38] for grasp model training in [13]. These 10 training sets have 8,988 grasps in total and 2308 out of these 8,988 grasps are successful grasps. We randomly select 5 sets (i.e. 4,578 grasp samples) out of the 10 training sets in [13] to train the initial grasp model for active learning. 1,168 out of these 4,578 grasps are successful grasps.

We run active learning to acquire 2,052 grasp queries in simulation. We online update the grasp model for each round of active learning as described in Section V. We randomly select a Bigbird object for every 5 active learning queries in order to cover the object space well.

The average rewards, average running time, and number of plays of these three active learning arms can be seen from Table I. We empirically add a constant of 0.35, -0.05 , and 0.6 to the max success, max uncertainty, and exploration

²<https://dartsim.github.io/>

³https://robot-learning.cs.utah.edu/project/grasp_active_learning

arm respectively. The constant terms cause the rewards of different arms to be in a similar range. The constant terms are supposed to make the rewards of different arms inside a similar range. We use the actively learned grasp model for grasp inference.

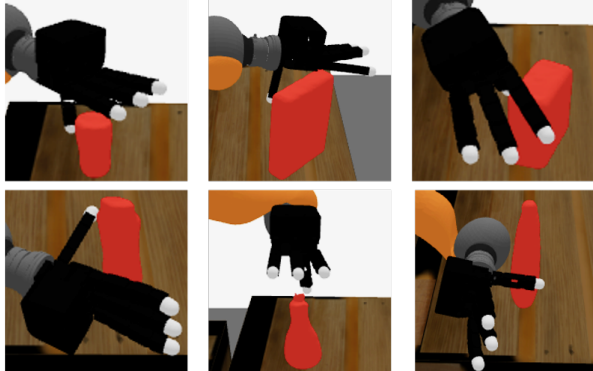


Fig. 3: Examples of grasp preshapes queries generated by our three active learning arms. The columns from left to right show grasp queries synthesized by the max success, max uncertainty, and the exploration arm respectively.

We show grasp preshapes generated by our active learning arms in Figure 3. The max success arm tends to generate grasp preshapes that leads to successful grasps with relatively large contact areas. The max uncertainty arm tends to synthesize grasps the voxel-based classifier is uncertain about. The exploration arm explores grasps with a low probability of seen in the training data (e.g. grasps relatively far away from the object).



Fig. 4: Active grasp preshape examples that the heuristic grasp planner during data collection is not able to generate.

Our heuristic grasp planner generates the palm pose of the grasp preshape for a given object in a heuristic and geometrical way with random Gaussian noises added [8]. It generates the joint angles of the grasp preshape by randomly sampling within a heuristic fixed range. Therefore, the heuristic grasp planner plans grasps in a limited grasping configuration subspace. Our active learner, especially the exploration arm, is able to generate grasps beyond the grasping configuration subspace of the heuristic grasp planner, which increases the grasping data diversity and covers more grasping configuration space. In Figure 4, we show active learning grasp preshape examples beyond the heuristic grasping configuration subspace, which our heuristic grasp planner is not able to generate.

We demonstrate the active learning grasping data has a larger diversity than the heuristic grasping data by computing

	Active learning	Heuristic mean	Heuristic std
Config entropy	-6.1	-33.6	0.05
Pose entropy	0.1	-1.5	0.05
Joint entropy	-6	-32.1	0.007

TABLE II: The differential entropy of multivariate Gaussian distributions fit to active learning and heuristic grasping data.

the Shannon differential entropy of multivariate Gaussian distribution fit to the grasping data. In information theory, the entropy is a quantity that interprets the average level of information or uncertainty inherent in the variable’s possible outcomes [39]. Entropy is a reasonable measure of data diversity [40, 41]. The more different data samples there are, and the more evenly data samples distributes, the more information or uncertainty there is in the data, and the larger the entropy of the data is. We fit a multivariate Gaussian to the grasping data. We compute and report the differential entropy of the Gaussian distribution for both active learning and heuristic grasping data in Table II as our grasping diversity metric [42].

The grasp palm pose for entropy computation is in Cartesian space, while hand joint angles are in radians. We generate 4 heuristic grasp subsets by randomly selecting grasps from these 8,988 heuristic training grasps without replacement. Each subset has 2,052 heuristic grasps. Each heuristic grasp subset has the same number of grasps as the active learning data. The second column of Table II shows the entropy of active learning. The third and last column report the mean and standard deviation of the entropy across these 4 heuristic subsets. We report the grasp configuration, palm pose, and joint angle entropy of active learning and heuristic data in the second to last row of Table II. As we can see from Table II, the grasp configuration, palm pose, and joint angle entropy of the active learning data are larger than these of the heuristic data. This shows the active learning data has larger diversity than heuristic data.

C. Real Robot Experiments

We compare our active learning model with the initial passive supervised model to show if our active learner can improve the initial model. We also compare our active learning model with a passive supervised learning model trained with more heuristic grasping data. We use the 8,988 geometrical grasps collected in [13] to train the grasp model with more data in a passive supervised way. We use the same training specifications as [13] to train this passive supervised model with more training data.

We evaluate grasp planning as inference using the active learning model, the passive supervised model trained with 8,988 geometrical grasps, and the passive supervised initial model trained with 4,578 geometrical grasps on the physical robot system. We perform experiments on 8 YCB [43] objects covering different textures, shapes, and sizes. We show the experimental setup and objects used in Figure 5. All experimental objects are unseen in training except for “Pringles”. We attempted grasps at 5 different poses per



Fig. 5: Experimental setup with objects used for experiments. From left to right objects are “pringles”, “pitcher”, “soft scrub”, “sugar box”, “mustard bottle”, “Lego”, “soccer ball”, and “mug”. Objects range in size from $8 \times 9 \times 11$ cm (mug) to $13 \times 17 \times 24$ cm (pitcher).

object, for a total of 40 grasp attempts per method. We use the same set of locations across different methods, but each object has its own set of random poses. In total, we performed 120 grasp attempts for 3 different methods across 8 objects in this paper.

If the RRT-connect motion planner fails to generate a plan for a grasp due to collision avoidance, we generate a new grasp using the same grasp planner with a different initialization. If the grasp planner could not generate a grasp with a motion plan in 5 attempts, we treat the grasp attempt as a failure case. It turns out all three grasp planners can find a grasp with a feasible motion plan for every object pose we tested in 5 attempts.

As described in Section VI-A, we label a grasp attempt that successfully lifts the object to a height of 0.15m without dropping it as successful. We also manually label each experimented grasp to be a side or overhead grasp.

The grasp success rates for all three methods are summarized in Figure 6. It takes around 3 – 10 seconds for each method to generate a grasp. The grasp planners using the active learning model, the passive supervised model with more training data, and the passive supervised model for initialization achieve grasping success rates of 50%, 52.5%, and 32.5% respectively for the 8 objects.

The grasp inference using the active learning model generated 15 side and 25 overhead grasps for 8 testing objects. The grasp inference using the passive supervised model with more training data plans 11 side and 29 overhead grasps for the supervised planner with more training data. The grasp inference using the passive supervised model for initialization generated 14 side and 26 overhead grasps. More overhead grasps than side grasps are generated for all three grasp planners, which holds for both experiments and data collection. Overhead grasps are relatively further away from the table compared with side grasps, which makes it easier

	Active	Supervised more	Supervised less
Config entropy	-16.3	-18.6	-15.9
Pose entropy	-3.7	-4.2	-3.7
Joint entropy	-11.8	-13.5	-11

TABLE III: The differential entropy of the multivariate Gaussian distribution fit to our real-robot experiment grasps of these three different methods: active learning, supervised learning using more heuristic training data, and supervised learning using less heuristic data for initialization.

for the motion planner to avoid collision with the table for overhead grasps.

We reported the grasp success rates of side and overhead grasps separately for each grasp planner in Figure 6. The grasp inference using the active learning model, the passive supervised model with more training data, and the passive supervised model for initialization achieve success rates of 93.3%, 100%, and 78.6% respectively for side grasps of the 8 objects. The grasp inference using the active learning model, the passive supervised model with more training data, and the passive supervised model for initialization achieve success rates of 24%, 34.5%, and 7.7% respectively for overhead grasps of the 8 objects.

All three grasp planners have lower success rate for overhead grasps than side grasps. Objects such as mustard, mug, and lego have relatively smaller contact areas available for overhead grasps and our grasp controller would push them away when closing the hand as it had no feedback from vision or haptic sensors to know the object was moving [13]. All grasp planners are not able to plan any successful side grasps for the object mug. Only overhead grasps are planned for the object mug and all of them failed. Since the mug object is relatively short, the motion planner could not find paths which would not collide with the table for side grasps for all three methods.

The grasp planner using the active learning model outperforms the passive supervised model for initialization, which shows the active learning can improve the supervised passive model for grasp inference. The grasp planner using the active learning model achieves comparable performance with the passive supervised learning with fewer grasp samples, which demonstrates the benefit of grasp active learning. This implies that our active grasp learning covers the grasp configuration space better across different objects with fewer samples, compared with passive supervised grasp learning.

In Figure 7, example grasps are shown for different objects generated by our inference approach with the actively learned grasp model, including the voxel-based classifier and MDN prior. We show side grasps that provide stability in the top row. We present overhead grasps in the bottom row, which offer dexterity and access to objects in clutter.

We use the differential entropy of multivariate Gaussian distributions as the grasp diversity metric for grasping experiments, as in subsection VI-B. Table III shows the differential entropy of our real-robot experiment grasps of our three different methods: active learning, passive supervised learning

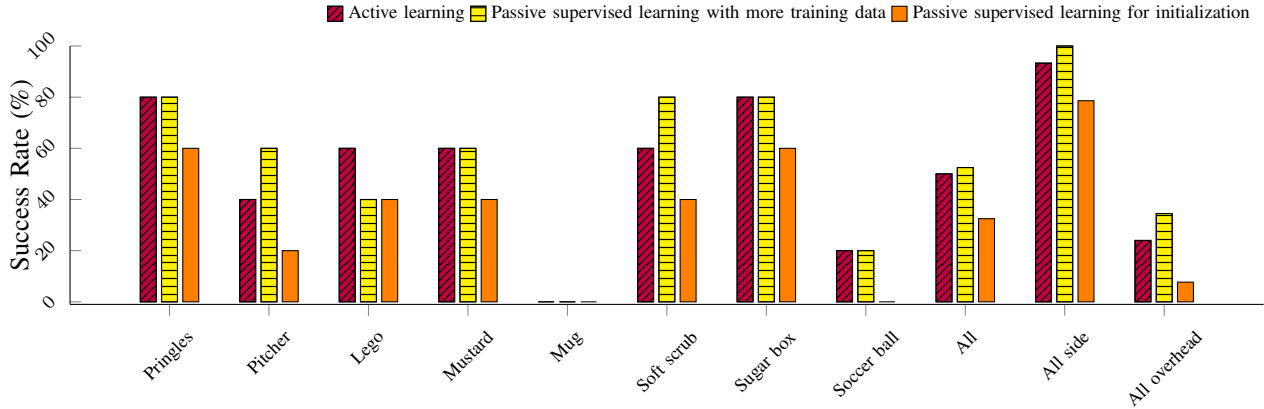


Fig. 6: Multi-fingered grasping success rates of grasp inference using 3 different models on the real robot. “Pringles” was seen in training, other 7 objects are previously unseen.



Fig. 7: Examples of successful grasps generated by inference with our actively learned grasp model classifier and object-conditional prior. The top row shows side grasps. The bottom row shows overhead grasps.

trained with more heuristic grasping data, and passive supervised learning for initialization trained with less heuristic data. We report the entropy of the grasp configuration, palm pose, and joint angle of these three methods in the second to last row of the table. As can be seen from Table III, our active learning experiment grasps have larger entropy than the experiment grasps of supervised learning trained with more heuristic data. This means our active learning plans real-robot grasps with more diversity than supervised learning using more heuristic data. The experiment grasps of supervised learning using less heuristic data have larger entropy than experiment grasps of our active learning, which shows supervised learning using less heuristic data generates grasps with larger diversity than our active learning. This is because supervised learning using less data has more low-quality failure grasps than active learning, which increases the diversity of the experiment grasps of the supervised learning using less data.

VII. DISCUSSION AND CONCLUSION

In this work, we propose three different active learning arms for grasping and formalize active learning as a multi-arm bandit problem. Our real-robot grasping experiment shows our active grasp planner using less training data

achieves comparable success rates with a passive supervised planner trained with geometrical grasping data. This implies our active grasp learning covers the grasp configuration space better across different objects with fewer samples, compared with passive supervised grasp learning. We also compute the differential entropy to demonstrate our active learner generates grasps with larger diversity than passive supervised learning using more heuristic data, which attains comparable success rate.

In the future, we will run more rounds of active learning in order to cover more of the grasping and objects space, which can help to generate grasps with more diversities for different tasks. We plan to compare our query synthesis grasp active learning with pooling-based active learning. We think learning or designing a more complex feedback controller for overhead grasps using tactile feedback would boost the overhead grasp performance [13].

REFERENCES

- [1] J. Bohg, A. Morales, T. Asfour, and D. Kragic, “Data-Driven Grasp Synthesis—a Survey,” *IEEE Trans. on Robotics*, vol. 30, no. 2, pp. 289–309, 2014.
- [2] A. Saxena, J. Driemeyer, and A. Y. Ng, “Robotic Grasping of Novel Objects using Vision,” *Intl. Journal of Robotics Research*, vol. 27, no. 2, pp. 157–173, 2008.

- [3] A. Saxena, L. L. S. Wong, and A. Y. Ng, "Learning Grasp Strategies with Partial Shape Information," in *AAAI National Conf. on Artificial Intelligence*, 2008, pp. 1491–1494.
- [4] I. Lenz, H. Lee, and A. Saxena, "Deep Learning for Detecting Robotic Grasps," *Intl. Journal of Robotics Research*, vol. 34, no. 4-5, pp. 705–724, 2015.
- [5] L. Pinto and A. Gupta, "Supersizing Self-supervision: Learning to Grasp from 50K Tries and 700 Robot Hours," in *IEEE Intl. Conf. on Robotics and Automation*, 2016, pp. 3406–3413.
- [6] M. Kopicki, R. Detry, M. Adjigble, R. Stolkin, A. Leonardis, and J. L. Wyatt, "One-Shot Learning and Generation of Dexterous Grasps for Novel Objects," *Intl. Journal of Robotics Research*, vol. 35, no. 8, pp. 959–976, 2016.
- [7] J. Mahler, J. Liang, S. Niyaz, M. Laskey, R. Doan, X. Liu, J. A. Ojea, and K. Goldberg, "Dex-Net 2.0: Deep Learning to Plan Robust Grasps with Synthetic Point Clouds and Analytic Grasp Metrics," in *Robotics: Science and Systems*, 2017.
- [8] Q. Lu, K. Chenna, B. Sundaralingam, and T. Hermans, "Planning Multi-Fingered Grasps as Probabilistic Inference in a Learned Deep Network," in *Intl. Symp. on Robotics Research*, 2017.
- [9] A. Mousavian, C. Eppner, and D. Fox, "6-dof graspnet: Variational grasp generation for object manipulation," *arXiv preprint arXiv:1905.10520*, 2019.
- [10] A. Sahbani, S. El-Khoury, and P. Bidaud, "An Overview of 3D Object Grasp Synthesis Algorithms," *Robotics and Autonomous Systems*, vol. 60, no. 3, pp. 326–336, 2012.
- [11] J. Varley, J. Weisz, J. Weiss, and P. Allen, "Generating Multi-Fingered Robotic Grasps via Deep Learning," in *IEEE/RSJ Intl. Conf. on Intelligent Robots and Systems*, 2015, pp. 4415–4420.
- [12] M. Veres, M. Moussa, and G. W. Taylor, "Modeling Grasp Motor Imagery through Deep Conditional Generative Models," *IEEE Robotics & Automation Letters*, vol. 2, no. 2, pp. 757–764, 2017.
- [13] Q. Lu, M. Van der Merwe, B. Sundaralingam, and T. Hermans, "Multi-fingered grasp planning via inference in deep neural networks," *IEEE Robotics & Automation Magazine*, 2020.
- [14] S. Levine, P. Pastor, A. Krizhevsky, J. Ibarz, and D. Quillen, "Learning Hand-Eye Coordination for Robotic Grasping with Deep Learning and Large-Scale Data Collection," *Intl. Journal of Robotics Research*, p. 0278364917710318, 2016.
- [15] C. Eppner, A. Mousavian, and D. Fox, "A billion ways to grasp: An evaluation of grasp sampling schemes on a dense, physics-based grasp data set," *arXiv preprint arXiv:1912.05604*, 2019.
- [16] B. Settles, *Active Learning*. Morgan & Claypool, 2012.
- [17] O. Kroemer, R. Detry, J. Piater, and J. Peters, "Combining active learning and reactive control for robot grasping," *Robotics and Autonomous Systems*, vol. 58, no. 9, pp. 1105–1116, 2010.
- [18] M. Laskey, J. Mahler, Z. McCarthy, F. T. Pokorny, S. Patil, J. Van Den Berg, D. Kragic, P. Abbeel, and K. Goldberg, "Multi-armed bandit models for 2d grasp planning with uncertainty," in *IEEE Intl. Conf. on Automation Science and Engineering*, 2015, pp. 572–579.
- [19] J. Mahler, F. T. Pokorny, B. Hou, M. Roderick, M. Laskey, M. Aubry, K. Kohlhoff, T. Kröger, J. Kuffner, and K. Goldberg, "Dex-net 1.0: A cloud-based network of 3d objects for robust grasp planning using a multi-armed bandit model with correlated rewards," in *IEEE Intl. Conf. on Robotics and Automation*, 2016, pp. 1957–1964.
- [20] Q. Lu and T. Hermans, "Modeling Grasp Type Improves Learning-Based Grasp Planning," *IEEE Robotics & Automation Letters*, 2019.
- [21] M. Gualtieri, A. ten Pas, K. Saenko, and R. Platt, "High Precision Grasp Pose Detection in Dense Clutter," in *IEEE/RSJ Intl. Conf. on Intelligent Robots and Systems*, 2016, pp. 598–605.
- [22] E. Johns, S. Leutenegger, and A. J. Davison, "Deep Learning a Grasp Function for Grasping under Gripper Pose Uncertainty," in *IEEE/RSJ Intl. Conf. on Intelligent Robots and Systems*, 2016, pp. 4461–4468.
- [23] J. Redmon and A. Angelova, "Real-Time Grasp Detection using Convolutional Neural Networks," in *IEEE Intl. Conf. on Robotics and Automation*, 2015, pp. 1316–1322.
- [24] S. Kumra and C. Kanan, "Robotic Grasp Detection using Deep Convolutional Neural Networks," in *IEEE/RSJ Intl. Conf. on Intelligent Robots and Systems*, 2017.
- [25] D. Kalashnikov, A. Irpan, P. Pastor, J. Ibarz, A. Herzog, E. Jang, D. Quillen, E. Holly, M. Kalakrishnan, V. Vanhoucke *et al.*, "Qt-opt: Scalable deep reinforcement learning for vision-based robotic manipulation," *arXiv preprint arXiv:1806.10293*, 2018.
- [26] B. Wu, I. Akinola, A. Gupta, F. Xu, J. Varley, D. Watkins-Valls, and P. K. Allen, "Generative attention learning: a general framework for high-performance multi-fingered grasping in clutter," *Autonomous Robots*, pp. 1–20, 2020.
- [27] C. Ferrari and J. Canny, "Planning optimal grasps," in *IEEE Intl. Conf. on Robotics and Automation*. IEEE, 1992, pp. 2290–2295.
- [28] M. Ciocarlie, C. Goldfeder, and P. Allen, "Dimensionality Reduction for Hand-Independent Dexterous Robotic Grasping," in *IEEE/RSJ Intl. Conf. on Intelligent Robots and Systems*, 2007, pp. 3270–3275.
- [29] A. Morales, E. Chinellato, A. H. Fagg, and A. P. del Pobil, "An active learning approach for assessing robot grasp reliability," in *IEEE/RSJ Intl. Conf. on Intelligent Robots and Systems*, 2004, pp. 485–490.
- [30] L. Montesano and M. Lopes, "Active learning of visual descriptors for grasping using non-parametric smoothed beta distributions," *Robotics and Autonomous Systems*, vol. 60, no. 3, pp. 452–462, 2012.
- [31] X. Fu, Y. Liu, and Z. Wang, "Active learning-based grasp for accurate industrial manipulation," *IEEE Transactions on Automation Science and Engineering*, 2019.
- [32] H. Tian, C. Wang, D. Manocha, and X. Zhang, "Transferring Grasp Configurations using Active Learning and Local Replanning," *arxiv*, 2018.
- [33] M. Laskey, Z. McCarthy, J. Mahler, F. T. Pokorny, S. Patil, J. Van Den Berg, D. Kragic, P. Abbeel, and K. Goldberg, "Budgeted multi-armed bandit models for sample-based grasp planning in the presence of uncertainty," in *IEEE Intl. Conf. on Robotics and Automation*, 2015.
- [34] J. Oberlin and S. Tellex, "Autonomously acquiring instance-based object models from experience," in *Intl. Symp. on Robotics Research*, 2015, pp. 73–90.
- [35] C. Eppner and O. Brock, "Visual detection of opportunities to exploit contact in grasping using contextual multi-armed bandits," in *IEEE/RSJ Intl. Conf. on Intelligent Robots and Systems*, 2017, pp. 273–278.
- [36] D. A. Cohn, "Neural network exploration using optimal experiment design," in *Advances in neural information processing systems*, 1994, pp. 679–686.
- [37] Y. Gal, R. Islam, and Z. Ghahramani, "Deep bayesian active learning with image data," in *Intl. Conf. on Machine Learning*, 2017.
- [38] A. Singh, J. Sha, K. S. Narayan, T. Achim, and P. Abbeel, "Bigbird: A Large-Scale 3D Database of Object Instances," in *IEEE Intl. Conf. on Robotics and Automation*, 2014, pp. 509–516.
- [39] C. E. Shannon, "A mathematical theory of communication," *Bell system technical journal*, vol. 27, no. 3, pp. 379–423, 1948.
- [40] L. Jost, "Entropy and diversity," *Oikos*, vol. 113, no. 2, pp. 363–375, 2006.
- [41] I. F. Spellerberg and P. J. Fedor, "A tribute to claudes shannon (1916–2001) and a plea for more rigorous use of species richness, species diversity and the shannon-wiener index," *Global ecology and biogeography*, vol. 12, no. 3, pp. 177–179, 2003.
- [42] N. A. Ahmed and D. Gokhale, "Entropy expressions and their estimators for multivariate distributions," *IEEE Transactions on Information Theory*, vol. 35, no. 3, pp. 688–692, 1989.
- [43] B. Calli, A. Singh, A. Walsman, S. Srinivasa, P. Abbeel, and A. M. Dollar, "The YCB Object and Model Set: Towards Common Benchmarks for Manipulation Research," in *Intl. Conf. on Advanced Robotics*, 2015, pp. 510–517.